versatility of this vapor-transport approach. As expected, the germanium nanowires grow at an inclined angle on a non-germanium (111) substrate due to crystallographic mismatch. We demonstrate the feasibility of controlled synthesis of individual vertical semiconducting germanium nanowires. These nanowires can be directly integrated into fabricated devices[1,2] to produce nanoscale vertical transistors. Other applications for individual vertical germanium nanowires or arrays of high-density germanium nanowires include terapixel infrared photodetection systems, memory devices with metal oxide/semiconductor structures and germanium nanowires, germanium-based cryogenic power electronics for deep-space exploration, and monolithic germanium nanoresonators. Large-scale synthesis of functionalized germanium nanostructures may find chemotherapeutic applications in nanomedicine, as certain germanium compounds exhibit low mammalian toxicity but marked activity against certain bacteria. Other applications may include high-sensitivity functionalized biosensors or catalysts for nanoelectroplating. Germanium oxide is a photoluminescent material with peak energies at 3.1 eV and 2.2 eV. Oxidation of the germanium nanowires can produce germanium oxide nanowires for photoluminescence studies and optoelectronic applications.

Experimental

Doped and intrinsic germanium(III) substrates were coated with poly(methyl methacrylate) (PMMA, 950 kg mol^{-1} relative molecular mass, 2 wt.-% in chlorobenzene, spin-coated at 5000 rpm and 200 °C, with a post-bake), exposed with an electron beam (Hitachi H-700, 600–700 μC cm^{-2}, 30 kV), and developed with methyl isobutyl ketone/isopropanol (1:3 v/v, 30 s, 23 °C, 20–30 s isopropanol rinse). Gold (99.95 % metal basis) was deposited by ion-beam sputtering technology, and the resist lift-off process was performed in acetone (1–2 min, sonication, 23 °C).

The germanium nanowires were synthesized using the gold catalyst-mediated homoepitaxial growth approach in a dual-zone tubular reaction chamber setup. The source, composed of a 1:1 weight ratio of germanium powder (Alfa Aesar, 99.999 % metal basis) and synthetic graphite powder (Alfa Aesar, 99.9995 % metal basis), was placed upstream of the substrate. The graphite additive provides enhanced surface area for the evaporation of germanium at elevated temperature and control of the germanium partial pressure at a given carrier gas flow rate and fixed source temperature. Graphite also reduces the amount of germanium oxide (native oxide on the as-purchased germanium powder) by carbothermal reduction. Thermodynamic considerations [3] suggest that formation of crystalline germanium carbide nanowires is highly unlikely due to the disproportionate heats of formation of gaseous carbon and germanium species, the intrinsic metastability of the Ge–C bond compared with C–C bonds, and the thermodynamic insolubility of carbon in crystalline germanium at a wide range of temperatures and pressures. Uniform vertical nanowire growth was achieved at 1020–1030 °C source temperature, 470–480 °C substrate temperature, and a carrier gas of 100–140 sccm argon (Scott Specialty Gases, 99.999 % pure) and 50–80 sccm hydrogen (Scott Specialty Gases, 99.999 % pure). It is important to maximize germanium-vapor flux while maintaining a local environment conducive to growth of crystalline nanowires. The purpose of hydrogen introduction is to prevent and reverse any oxidation of gas-phase and solid-phase germanium by residual oxygen and carbon oxides in the gas system and to provide a passivation layer. The advantages of the dual-zone vapor transport process for nanowire growth compared to other methods [7–10], such as laser ablation and organometallic chemical vapor deposition, include a simpler reactor chamber setup, minimal equipment investments, and non-hazardous materials and gases. Scanning electron microscopy (SEM) was performed using a Hitachi S4000 field-emission SEM (20 kV, 15 μA). Transmission electron microscopy (TEM) analysis was performed using a Phillips CM20 TEM with an acceleration voltage of 200 kV, and X-ray photoelectron spectroscopy (XPS) analysis was performed using a SSI S-Probe Monochromatized XPS Spectrometer with an Al Kα (1486 eV) radiation probe.

Received: June 8, 2004
Final version: October 18, 2004

[1] H. T. Ng, J. Han, T. Yamada, P. Nguyen, Y. P. Chen, M. Meyyappan, *Nano Lett.* **2004**, *4*, 1247.
[2] P. Nguyen, H. T. Ng, T. Yamada, M. Smith, J. Li, J. Han, M. Meyyappan, *Nano Lett.* **2004**, *4*, 651.
[3] *CRC Handbook of Chemistry and Physics*, 78th ed. (Ed: D. R. Lide), CRC Press, Boca Raton, FL **1998**.
[4] S. M. Sze, *Physics of Semiconductor Devices*, 2nd ed., Wiley, New York **1981**.
[5] A. G. Cullis, L. T. Canham, P. D. J. Calcott, *J. Appl. Phys.* **1997**, *82*, 909.
[6] C. O. Chiu, H. Kim, P. C. McIntyre, K. C. Saraswat, *Tech. Dig.—Int. Electron Devices Meet.* **2003**, 437.
[7] A. M. Morales, C. M. Lieber, *Science* **1998**, *279*, 208.
[8] G. Gu, M. Burghard, G. T. Kim, G. S. Düsberg, P. W. Chiu, V. Krstic, S. Roth, W. Q. Han, *J. Appl. Phys.* **2001**, *90*, 5747.
[9] T. Hanrath, T. A. Korgel, *J. Am. Chem. Soc.* **2002**, *124*, 1424.
[10] T. I. Kamins, X. Li, R. S. Williams, X. Liu, *Nano Lett.* **2004**, *4*, 503.
[11] B. Messer, J. H. Song, P. Yang, *J. Am. Chem. Soc.* **2000**, *122*, 10 232.
[12] H. T. Ng, B. Chen, J. Li, J. Han, M. Meyyappan, J. Wu, S. X. Li, E. E. Haller, *Appl. Phys. Lett.* **2003**, *82*, 2023.
[13] P. Nguyen, H. T. Ng, J. Kong, A. M. Cassell, R. Quinn, J. Li, J. Han, M. McNeil, M. Meyyappan, *Nano Lett.* **2003**, *3*, 925.
[14] R. S. Wagner, W. C. Ellis, *Appl. Phys. Lett.* **1964**, *4*, 89.

Templated Self-Assembly: Formation of Folded Structures by Relaxation of Pre-stressed, Planar Tapes**

By *Mila Boncheva* and *George M. Whitesides**

This work demonstrates the first step in a strategy for generating three-dimensional (3D) structures based on the spontaneous folding of elastomeric tapes, fabricated in corrugated or crimped forms with defined, quasi-3D shapes, and patterned with liquid solder. Capillary interactions between the solder drops pull the structures into their final form. The ultimate objective of this strategy is to develop methods to fabricate 3D microelectronic structures in processes that use photolithography to fabricate planar patterned substructures.

[*] Prof. G. M. Whitesides, Dr. M. Boncheva
Department of Chemistry and Chemical Biology
Harvard University
Cambridge, MA 02138 (USA)
E-mail: gwhitesides@gmwgroup.harvard.edu

[**] This work was supported by the NSF (CHE-0101432) and DARPA.

 DOI: 10.1002/adma.200400940 © 2005 WILEY-VCH Verlag GmbH & Co. KGaA, Weinheim

ADVANCED MATERIALS

Microfabrication of 3D structures using conventional projection lithography builds structures layer-by-layer in stacked, registered, planar sheets;[1–3] this process is versatile and very highly developed, but restricted to specific types of structures. We and others have begun to investigate self-assembly as a method for fabricating 3D microstructures.[4] Unconstrained self-assembly—i.e., self-assembly that proceeds without templates or geometrical restrictions—has, so far, only been demonstrated to generate regular, crystal-like structures. Constraining the self-assembly—by connecting the components in strings, or by limiting the volume in which the self-assembly occurs[5]—offers routes to a wider range of structures. Using components that were connected in a string, we have generated asymmetrical 3D structures and structures having regions with different electronic function;[6] this strategy is loosely based on the folding of proteins and RNAs into compact, functional, 3D structures.[7] Fabricating, patterning, and connecting the required components, however, included at least one manual step; thus, the sizes of the individual components, and the sizes of the resultant structures, were limited to the millimeter scale, and the procedure, however interesting, is not practical for fabricating microelectronic systems.

We and others have previously reported a procedure based on spontaneous folding which uses planar substrates to fabricate 3D polyhedra.[4,8] In this procedure, the substrates were patterned while flat, and were pulled into their 3D shapes by spontaneous folding caused by capillary forces. Here we explore an alternative process in which a tape is fabricated in a crimped form, stretched flat for patterning, and then allowed to relax back into the crimped form for self-assembly (Fig. 1). The final consolidation of these structures also results from capillary interactions between drops of molten solder. These two strategies have, so far, been applied only to model systems (e.g., systems without microelectronic function), and are intended to define their relative strengths and weaknesses. We believe, however, that they will ultimately be applicable to the fabrication of 3D structures with microelectronic functionality having geometries that are difficult to fabricate using other techniques.

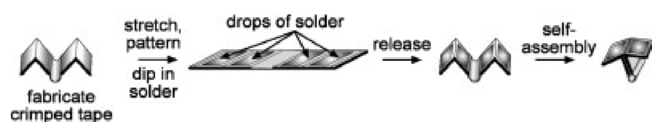

Figure 1. Scheme illustrating the experimental strategy used in this work.

Figure 2 outlines the experimental procedure (for details, see Experimental section). We fabricated the crimped tapes of poly(dimethylsiloxane) (PDMS) using replica molding in PDMS molds as previously described[9] (Figs. 2a–c). The tapes consisted of alternating regions of different thickness, and thereby, different flexibility. These tapes were oriented perpendicular to the plane of the PDMS molds. After releasing the tapes from the molds, we stretched them flat on a solid support (Figs. 2d,e). The stretching affected primarily the dimensions and shape of the thin, flexible hinge regions. We patterned the flattened tapes with metal features, which we subsequently covered with solder using dip-coating (Fig. 2f). When released from the support onto which they were flattened, the tapes spontaneously returned to the crimped shape in which they were fabricated (Fig. 2g). We placed the tapes in a container filled with water heated to a temperature above the melting temperature ($T_m = 47\,^\circ C$) of the solder, and agitated the suspension (Fig. 2h). While moving in the aqueous medium, the tapes bent in the flexible thin regions; this bending brought the less flexible, thicker regions into close proxim-

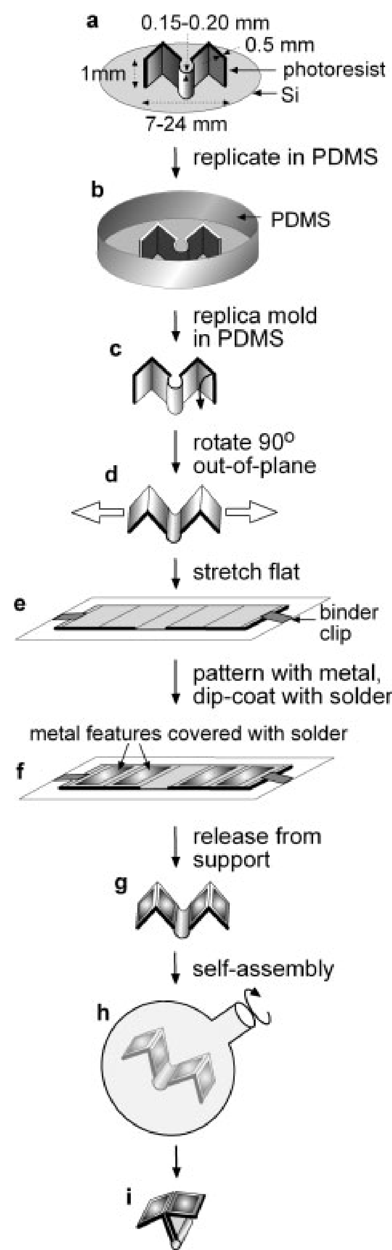

Figure 2. Fabrication, patterning, and self-assembly of crimped, elastomeric tapes. See Experimental section for details.

 © 2005 WILEY-VCH Verlag GmbH & Co. KGaA, Weinheim

ity. When droplets of molten solder patterned on adjacent rigid regions of the tapes came into contact, they fused; the fusion minimized the area of the solder–water interface, and thus its interfacial free energy. After folding was complete, cooling the suspension allowed the solder to harden, and generated mechanically stable structures (Fig. 2i).

Figure 3 shows examples of several structures fabricated using this strategy. The crimped shape of the tape and the pattern of drops of solder determined the geometry of the structure formed upon self-assembly. In the simplest case, the overall topology of the crimped tape remained unchanged upon self-assembly (Fig. 3a). Fusion of the drops of solder patterned on the crimped tape served only to consolidate the five-membered ring of thick PDMS features into a stable, quasi-3D structure. In other examples, we designed the crimped tapes such that the self-assembly resulted in formation of structures with new topology. Linear crimped tapes folded into curved (Fig. 3b) or closed circular (Fig. 3c) quasi-3D structures. We also demonstrated that folding of a linear crimped tape could lead to formation of a true 3D structure (Fig. 3d). The geometry of the linear tape designed to fold into a helix was similar to the one designed to fold into a closed circular structure (Fig. 3c) the angle between the rigid features (60°) was set to fit a six-membered closed ring (of the geometry shown in Fig. 3c), but the tape contained eight pairs of rigid elements instead of six. The flexibility of the thin regions allowed the tape to bend out-of-plane, and initiate the formation of a 3D helical structure.

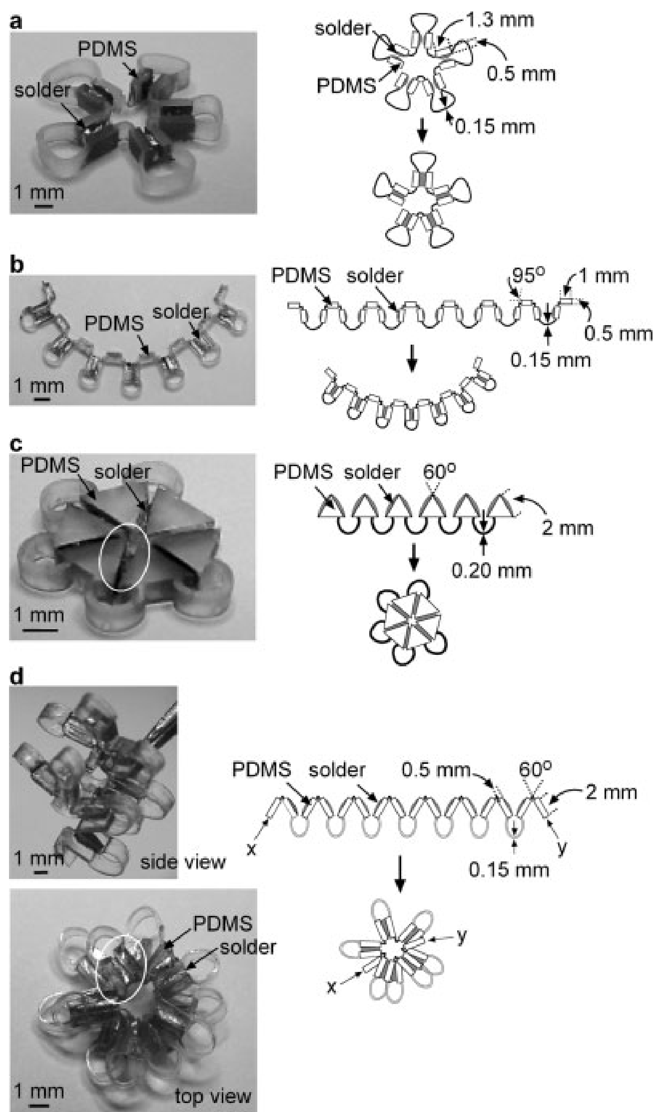

Figure 3. Photographs of quasi-3D (a–c) and true 3D (d) structures self-assembled from crimped elastomeric tapes. The schemes to the right of each photograph show the structure of the tape before (top) and after (bottom) folding. The white circles in (c) and (d) indicate defects in the folded structures caused by an excessive amount of solder deposited on the metal features.

Three characteristics of the crimped tapes were crucial for their successful folding into the target structures: i) The length of the flexible regions, ii) their thickness, and iii) the amount of solder deposited on the rigid parts. The length of the flexible regions of the tapes had to allow close contacts between adjacent rigid components during self-assembly, but prevent undesired non-nearest-neighbor contacts. The thickness of these regions had to be chosen such that the tapes would be able to bend in-plane or out-of-plane during self-assembly, and would not twist along their length. We chose the length and the thickness of the tapes empirically. They folded correctly into the target structures in all of the systems studied, without twisting, and without undesired contacts between non-adjacent parts of the tapes.

The only defect that we observed in the folded structures was due to the amount of solder deposited on the metal features: sides of the tapes that we have designed to be parallel assembled instead at an angle when the drops of solder connecting them were too large (see, for example, Figs. 3c,d). We controlled the amount of solder deposited on the metal features by the temperature at which we dip-coated the tapes: since the contact angle between the molten solder and the underlying metal is inversely proportional to the temperature of the solder,[10] we performed the dip-coating at a temperature considerably higher than the melting temperature of the solder $T_m = 47\,°C$ (approximately at 90 °C). This mechanism of control, however, proved insufficient: small variations in the contact angle (brought about, we believe, by the presence of impurities, e.g., oxides, on the surface of the solder) sometimes led to the deposition of larger quantities of solder than intended. Better control of the conditions during dip-coating (e.g., reduction of oxide formation by working under anaerobic conditions) would be needed to ensure that the right amount of solder covered the metal features. The amount of solder can also be optimized by reducing the width of the metal features,[4] or by using patterns comprising several small features instead of a single, large one; work intended to clarify these aspects of design is currently in progress.

Our main objective in this work was to demonstrate that linear tapes—correctly crimped and patterned with solder—can fold into 3D structures. We believe that the scope of struc-

 © 2005 WILEY-VCH Verlag GmbH & Co. KGaA, Weinheim

tures possible to achieve using this strategy is not limited to the quasi-3D and helical structures we have shown here. Previous work on self-assembly of unconnected components (e.g., millimeter-sized spheres[11] and colloids[12]) has demonstrated that hierarchical and templated self-assembly generate a much broader range of 3D shapes than is possible in an unconstrained system. By analogy with these examples, we believe that correctly designed tapes will self-assemble into increasingly more complex structures, following a hierarchical plan. The methods of soft lithography used to fabricate the crimped tapes make it possible to fabricate tapes with a variety of shapes, dimensions, and symmetries;[9] the lateral dimensions of the tapes can, in principle, be scaled down to hundred(s) of micrometers.

We have demonstrated a new strategy for fabrication of 3D structures based on spontaneous folding. This strategy has three new features: i) The linear precursors (tapes) are orientated perpendicular to the support during fabrication, and in the plane of the support during patterning. Thus, sides of the tapes that are concealed during fabrication are made accessible for surface treatment and patterning; ii) The tapes are fabricated in crimped shapes that facilitate and direct their subsequent self-assembly; iii) The flexibility of the tapes enables reversible crimping and flattening (that is, transitions between quasi-2D and quasi-3D forms), and makes possible patterning and functionalization of both sides of the tapes. This strategy has the potential to generate structures with 3D topology by using a combination of 2D photolithography and templated self-assembly. Such structures may be worth considering for the fabrication of 3D, flexible electronic devices, e.g., microelectronic chips-in-a-stack containing memory and logic elements,[13] conformal electronic devices[14] (devices that can fit in irregularly shaped cavities), and optoelectronic systems[15] (e.g., 3D displays). If this strategy is to be applied to fabrication of functional structures, the tapes must be decorated with components with electronic or optical functionality (e.g., memory or logic elements, lenses, gratings). These components can be placed opposite to the side of the tapes that is patterned with solder, in the regions of higher thickness. Alternatively, the functional components might be placed on a second, flat tape; this tape could be attached to the crimped tape while it is stretched flat for patterning.

Experimental

Fabrication of the Tapes: We used the standard procedures of soft lithography as previously described [9]. Briefly, first we fabricated a bas-relief master of the desired pattern using photolithography with positive photoresist (SU-8 100). We placed this master in a Petri dish, covered it with liquid precursor of PDMS doped (approximately 1–2 % *w/w*) with silica gel, and cured the pre-polymer overnight at 60 °C. After carefully peeling the PDMS mold from the master, we treated it with silane vapor ((tridecafluoro-1,1,2,2-tetrahydrooctyl)-1-trichlorosilane from United Chemical Technologies, Inc.) under vacuum for at least 3 h. We filled the silanized PDMS mold with PDMS pre-polymer, and cured it thermally as above. To release the PDMS tapes from the mold in which they were fabricated, we dipped the mold containing the tapes in dichloromethane and subsequently, in ethanol (approximately 5 min in each solvent); we repeated this treatment several times. The PDMS mold (doped with silica gel) and the PDMS tapes contained in it swelled and contracted differently in the two solvents; after approximately 30 min, the PDMS tapes, crimped in a defined, quasi-3D geometry, were released from the mold. We dried the tapes overnight in air.

Patterning of the Tapes: We stretched the tapes flat on a solid support (typically, a glass slide silanized as described above), attached them using binder clips, and oxidized them for 60 s in a N_2 plasma. We placed a prefabricated PDMS membrane (of thickness approximately 100 μm, silanized as above) on top of the tapes; this membrane comprised holes corresponding to the desired pattern of solder. Using the membrane as a stencil, we screen-printed a layer of a commercial, mercapto-ester-containing polymer (TraCoat 15C, from Tra-Con, Inc.) onto the PDMS tapes, and cured the polymer under UV light (100 W) for 40 min. After peeling the membrane off the tapes, we deposited gold (100 nm) via thermal evaporation. The gold layer adhered strongly onto the areas of the tapes bearing patterns of sulfur-containing polymer, and only weakly to the remaining surface of the PDMS tapes; a stream of distilled water from a pipette sufficed to wash the gold layer off the unmodified PDMS surfaces. We covered the metal-bearing patterns with solder (LMA-117 from Small Parts, Inc., melting temperature 47 °C) using dip-coating as previously described [16]. When released from the glass slide on which they were attached, the tapes—now carrying patterns of solder—spontaneously returned to the crimped shape in which they were fabricated.

Self-Assembly: We placed each tape in a cylindrical or a spherical container (typically, of volume 25–50 mL) filled with distilled water. The pH of the water was adjusted to 3 with HCl to dissolve oxides formed on the surface of the solder; the water also contained a drop of detergent (Triton-X) to prevent formation of air bubbles on the walls of the container and on the tapes. We heated the water to a temperature above the melting temperature of the solder (approximately 60 °C) using a heat gun, and agitated the container using the motor of a rotary evaporator (approximate rate of rotation 45 rpm). Collisions between neighboring features carrying droplets of molten solder led to fusion of the droplets due to capillary interactions, and to folding the tapes into the target structures. Cooling of the suspension to room temperature solidified the solder and gave mechanical stability to the structures. We performed each self-assembly experiment 3–4 times. All structures folded correctly in their target shapes. In all cases, folding of the structures occurred within 2–3 min.

Received: June 12, 2004
Final version: September 3, 2004

[1] S. A. Campbell, *The Science and Engineering of Microelectronic Fabrication*, 2nd ed., Oxford University Press, New York **2001**.
[2] W. M. Moreau, *Semiconductor Lithography: Principles, Practices, and Materials*, Plenum Press, New York **1988**.
[3] G. T. A. Kovacs, *Micromachined Transducers Sourcebook*, McGraw-Hill, New York **1998**.
[4] R. R. A. Syms, E. M. Yeatman, V. M. Bright, G. M. Whitesides, *J. Microelectromech. Syst.* **2003**, *12*, 387.
[5] M. Boncheva, G. M. Whitesides, in *Encyclopedia of Nanoscience and Nanotechnology* (Eds: J. A. Schwarz, C. Contescu, K. Putyera), Marcel Dekker, New York **2004**, p. 287.
[6] M. Boncheva, D. H. Gracias, H. O. Jacobs, G. M. Whitesides, *Proc. Natl. Acad. Sci. USA* **2002**, *99*, 4937.
[7] B. Alberts, D. Bray, J. Lewis, M. Raff, K. Roberts, J. D. Watson, *Molecular Biology of the Cell*, 3rd ed., Garland, New York **1994**.
[8] D. H. Gracias, V. Kavthekar, J. C. Love, K. E. Paul, G. M. Whitesides, *Adv. Mater.* **2002**, *14*, 235.
[9] Y. Xia, G. M. Whitesides, *Angew. Chem. Int. Ed.* **1998**, *37*, 550.
[10] J. S. Hwang, *Modern Solder Technology for Competitive Electronics Manufacturing*, McGraw-Hill, New York **1996**.

 © 2005 WILEY-VCH Verlag GmbH & Co. KGaA, Weinheim

[11] H. Wu, V. R. Thalladi, S. Whitesides, G. M. Whitesides, *J. Am. Chem. Soc.* **2002**, *124*, 14 495.
[12] Y. Yin, Y. Lu, B. Gates, Y. Xia, *J. Am. Chem. Soc.* **2001**, *123*, 8718.
[13] *Foldable Flex and Thinned Silicon Multichip Packaging Technology* (Ed: J. W. Balde), Kluwer Academic Publishers, Boston, MA **2003**.
[14] Y.-L. Loo, T. Someya, K. W. Baldwin, Z. Bao, P. Ho, A. Dodabalapur, H. E. Katz, J. A. Rogers, *Proc. Natl. Acad. Sci. USA* **2002**, *99*, 10 252.
[15] J. A. Rogers, Z. Bao, K. Baldwin, A. Dodabalapur, B. Crone, V. R. Raju, V. Kuck, H. Katz, K. Amundson, J. Ewing, P. Drzaic, *Proc. Natl. Acad. Sci. USA* **2001**, *98*, 4835.
[16] D. H. Gracias, J. Tien, T. L. Breen, C. Hsu, G. M. Whitesides, *Science* **2000**, *289*, 1170.

Incorporation of Highly Dispersed Gold Nanoparticles into the Pore Channels of Mesoporous Silica Thin Films and Their Ultrafast Nonlinear Optical Response**

By *Jin-Lou Gu*, *Jian-Lin Shi*,* *Guan-Jun You*, *Liang-Ming Xiong*, *Shi-Xiong Qian*, *Zi-Le Hua*, and *Hang-Rong Chen*

Due to their ultrafast optical response and large third-order nonlinear optical susceptibility, solid dielectric matrices embedded with metallic nanoparticles have been widely studied and have sparked great interest in various fields, such as telecommunications, optical-data storage, and information processing.[1] However, the fabrication of these kinds of composite films remains unsatisfactory, largely due to the difficulties in achieving a high enough metal content by the conventional melt-quenching method.[2] Although a wide variety of alternative routes, such as ion implantation,[3] sputtering,[4] and the sol–gel process[5] have been used to solve these difficulties, the embedded metal nanomaterials usually suffer from a comparatively wide size distribution and a considerable agglomeration, especially during high-temperature treatment. The synthesis of high-quality composite films with a high content of highly dispersed, uniformly distributed, metallic nanoparticles is still a great challenge.

Recently, periodic mesoporous materials have been used as molds for the growth of different metals with controlled size and morphology. These provide an ideal route to optimize the space filling of a solid porous matrix with metallic nanoparticles.[6,7] They can also act as templates for the synthesis of periodic nanoparticle arrays to study collective effects.[8] In fact, to meet practical optical needs, mesoporous thin films (MTFs) are preferred since they can be integrated into existing structures, such as waveguides.[9] However, up till now, the preparation of nanostructured metal within MTFs has not been greatly explored.[8,10] Herein, a facile and flexible strategy has been developed to incorporate uniformly and highly dispersed gold nanoparticles into the channels of MTFs.

The synthetic protocol combined a surface-modification scheme with a neutralization reaction to introduce Au-inorganic-compound precursor into the channels of MTFs as shown in Scheme 1. Using *N*-[3-(trimethoxysilyl)propyl]ethylene diamine (TPED) or aminopropyltrimethoxysilane (APS)

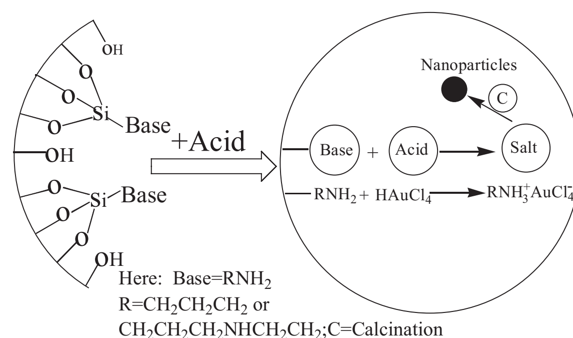

Scheme 1. Pictorial representation of the strategy to incorporate gold nanoparticles into the pore channels of MTFs.

to react with Si–OH groups on the internal pore surfaces, basic NH_2 moieties could be effectively grafted onto the mesochannels of MTFs.[11] After $HAuCl_4$ was introduced by a neutralization reaction,[12] followed by a reduction procedure,[7b] highly dispersed and uniformly distributed Au nanoparticles could be formed within the MTFs.

The assembly process was investigated by Fourier-transform infrared (FTIR) and UV-vis spectroscopy. The strong IR absorption at 2900–3000 cm^{-1}, assigned to the C–H bonds in the surfactant, can be clearly observed for the as-synthesized films. After extraction, these peaks are almost undetectable, which indicates that the surfactant has been removed from the MTFs. The disappearance of the absorption peak at 960 cm^{-1}, arising from the Si–OH bonds, accompanied by the appearance of the absorption of C–H bonds at 2900–3000 cm^{-1}, again demonstrates that the pore surface has been functionalized with basic moieties of NH_2.[11] Figure 1 shows the UV-vis absorption of a $HAuCl_4$ aqueous solution and of composite films with $HAuCl_4$

[*] Prof. J.-L. Shi, Dr. J.-L. Gu, Dr. L.-M. Xiong, Dr. Z.-L. Hua, Dr. H.-R. Chen
State Key Lab of High Performance Ceramics and Superfine Microstructure
Shanghai Institute of Ceramics
Chinese Academy of Science
1295 Dingxi Road, Shanghai, 200050 (P.R. China)
E-mail: jlshi@sunm.shcnc.ac.cn
Dr. G.-J. You, Prof. S.-X. Qian
State Key Lab of Applied Surface Physics
Physics Department, Fudan University
220 Handan Road, Shanghai, 200433 (P.R. China)

[**] This work was supported by the National Project for Fundamental Research (Grant No.2002CB613300), the National Natural Science Foundation of China (Grant No.50232050), and the National Hi-Tech Project of China (Grant No. 2002AA321010O).

DOI: 10.1002/adma.200401085
© 2005 WILEY-VCH Verlag GmbH & Co. KGaA, Weinheim